polymers

MDPI

Article

Synthesis, Characterization, and Proton Conductivity of Muconic Acid-Based Polyamides Bearing Sulfonated Moieties

Carlos Corona-García [1], Alejandro Onchi [1], Arlette A. Santiago [2], Tania E. Soto [3], Salomón Ramiro Vásquez-García [4], Daniella Esperanza Pacheco-Catalán [5] and Joel Vargas [1,*]

[1] Instituto de Investigaciones en Materiales, Unidad Morelia, Universidad Nacional Autónoma de México, Antigua Carretera a Pátzcuaro No. 8701, Col. Ex Hacienda de San José de la Huerta, Morelia C.P. 58190, Michoacán, Mexico; carcor93@gmail.com (C.C.-G.); alejandro.onchi@gmail.com (A.O.)
[2] Escuela Nacional de Estudios Superiores, Unidad Morelia, Universidad Nacional Autónoma de México, Antigua Carretera a Pátzcuaro No. 8701, Col. Ex Hacienda de San José de la Huerta, Morelia C.P. 58190, Michoacán, Mexico; arlette_santiago@enesmorelia.unam.mx
[3] Centro de Investigaciones Químicas, Instituto de Investigación en Ciencias Básicas y Aplicadas, Universidad Autónoma del Estado de Morelos, Av. Universidad 1001, Cuernavaca C.P. 62209, Morelos, Mexico; tania.soto@uaem.mx
[4] Facultad de Ingeniería Química, Universidad Michoacana de San Nicolás de Hidalgo, General Francisco J. Múgica s/n, Morelia C.P. 58060, Michoacán, Mexico; salomon_vg@yahoo.com
[5] Unidad de Energía Renovable, Centro de Investigación Científica de Yucatán, A.C. Carretera Sierra Papacal-Chuburná Puerto Km 5, Sierra Papacal, Mérida C.P. 97302, Yucatán, Mexico; dpacheco@cicy.mx
* Correspondence: jvargas@iim.unam.mx; Tel.: +52-443-147-7887

Abstract: Most commercially available polymers are synthesized from compounds derived from petroleum, a finite resource. Because of this, there is a growing interest in the synthesis of new polymeric materials using renewable monomers. Following this concept, this work reports on the use of muconic acid as a renewable source for the development of new polyamides that can be used as proton-exchange membranes. Muconic acid was used as a comonomer in polycondensation reactions with 4,4′-(hexafluoroisopropylidene)bis(*p*-phenyleneoxy)dianiline, 2,5-diaminobencensulfonic acid, and 4,4′-diamino-2,2′-stilbenedisulfonic acid as comonomers in the synthesis of two new series of partially renewable aromatic–aliphatic polyamides, in which the degree of sulfonation was varied. Fourier transform infrared spectroscopy (*FTIR*) and nuclear magnetic resonance (^{1}H, ^{13}C, and ^{19}F-*NMR*) techniques were used to confirm the chemical structures of the new polyamides. It was also observed that the degree of sulfonation was proportional to the molar ratio of the diamines in the feed. Subsequently, membranes were prepared by casting, and a complete characterization was conducted to determine their decomposition temperature (T_d), glass transition temperature (T_g), density (ρ), and other physical properties. In addition, water uptake (W_u), ion-exchange capacity (*IEC*), and proton conductivity (σ_p) were determined for these membranes. Electrochemical impedance spectroscopy (*EIS*) was used to determine the conductivity of the membranes. MUFASA34 exhibited a σ_p value equal to 9.89 mS·cm^{-1}, being the highest conductivity of all the membranes synthesized in this study.

Keywords: muconic acid; renewable polyamide; sulfonated polymer; ionomer; proton-exchange membrane

Citation: Corona-García, C.; Onchi, A.; Santiago, A.A.; Soto, T.E.; Vásquez-García, S.R.; Pacheco-Catalán, D.E.; Vargas, J. Synthesis, Characterization, and Proton Conductivity of Muconic Acid-Based Polyamides Bearing Sulfonated Moieties. *Polymers* **2023**, *15*, 4499. https://doi.org/10.3390/polym15234499

Academic Editor: Abdel-Hamid I. Mourad

Received: 13 October 2023
Revised: 13 November 2023
Accepted: 16 November 2023
Published: 23 November 2023

1. Introduction

The switch to renewable energy and the use of renewable resources is challenging; thus, many industrial processes are designed to work with fossil resources. In addition, in the past, the polymer industry designed materials with the only purpose of meeting the needs and optimizing production costs. This led to several issues, such as environmental pollution and the excessive use of non-renewable resources, among others. Consequently, polymers that can be more easily recycled and that bear some renewable moieties in their structures are currently being investigated [1–3].

An alternative technology for clean energy production is the proton-exchange membrane fuel cell (PEMFCs); this device exhibits the qualities of a high power density, easy start-up, scalable size, and low temperature operation; its function is to convert the chemical energy of fuels (such as H_2, methanol, among others) directly into electrical energy using a proton-exchange membrane (PEM). The desired characteristics of PEMs are usually high proton conductivity; and thermal, chemical, and mechanical stability properties, not allowing the flow of reagents through the membrane and being economically accessible [4–7].

Accordingly, the PEM is one of the most important parts or PEMFCs. Nafion®, marketed by DuPont, is a sulfonated perfluorinated membrane used par excellence in PEMFCs; there are other similar membranes marketed by Dow and Asahi that have also been used as PEMs, however the cost of the membranes prepared from these ionomers is high due to the complicated production process, which limits the wide commercialization of these devices [7,8]. Due to the latter issue, two approaches can be considered to develop materials that can be used as PEMs: the first one is modifying the nafion to improve its properties, but this does not lower the cost of the membrane; the second one is synthesizing polymers with similar chemical structures. It is worth noting that significant progress in fuel cell development has also been made for aromatic polymer membranes [7,9–13] and acid-base blended proton-exchange membranes [14–16]. However, at present, almost all commercial synthetic polymers are derived from a small collection of petrochemical feedstocks [17].

In order to circumvent this issue, biomass is considered a very promising alternative to some compounds derived from fossil resources, and several polymers derived from renewable resources are currently being commercialized [18–21]. When superior mechanical and thermal properties are required, engineering polymers, such as polyamides (PAs), are preferred [22]; in this regard, some polyamides, which are synthesized from renewable raw materials, compete with their petroleum-derived counterparts from an economic perspective [17,22,23].

Muconic acid is a sustainable monomer obtained by biological routes, such as the biofermentation of sugar, lignin, or derivatives [24–29]. This compound is a high value-added product because it can be polymerized by different routes. The double bonds present in its structure make it possible to polymerize it by free radicals, while the presence of the two carboxylic acid groups allows polymerization by condensation in combination with diols or diamines [30]. In both types of polymerizations, the polymer backbone presents unsaturations, making it possible for these renewable-based materials to possess improved functionality in terms of their tunable chemical and mechanical properties [24,25,30,31].

Based on the abovementioned ideas, this research explores the synthesis and characterization of new sulfonated polyamides using muconic acid as a renewable comonomer in polycondensation reactions with 4,4′-(hexafluoroisopropylidene)bis(*p*-phenyleneoxy)dianiline (HFDA) and sulfonated diamine 2,5-diaminobencensulfonic acid (DABS) and 4,4′-diamino-2,2′-stilbenedisulfonic acid (DASDA) to produce two series of novel polyamides with a controlled degree of sulfonation, MUFABA and MUFASA, respectively. Their chemical structures are characterized by Fourier transform infrared (*FTIR*) and nuclear magnetic resonance (^{1}H, ^{13}C, ^{19}F-*NMR*) spectroscopies. Electrochemical impedance spectroscopy (*EIS*) is used to determine the proton conductivity of the membrane of new muconic acid-based polyamide membranes. To the best of our knowledge, the use of muconic acid to obtain sulfonated polyamides for proton-exchange membranes has not been investigated. Therefore, this research contributes to the field of green chemistry by providing a sustainable approach to deliver specialty polymer products for alternative energy technologies.

2. Materials and Methods

2.1. Characterization Techniques

A Bruker Avance III HD (Bruker, Hamburg, Germany) was employed to record ^{1}H-*NMR*, ^{13}C-*NMR*, and ^{19}F-*NMR* spectra at 400, 100, and 376 MHz, respectively. DMSO-d_6 was used as a solvent at a typical concentration of 0.1 g·mL^{-1}; hexafluorobenzene (HFB)

and tetramethylsilane (TMS) were used as internal standards in this analysis. A Thermo Scientific Nicolet iS10 FTIR spectrometer fitted with an ATR accessory with a diamond crystal was employed to collect 32 spectra and coded for each membrane at 1 × 1 cm and around 400 μm in thickness in a range of 4000 to 650 cm^{-1} at a spectral resolution equal to 4 cm^{-1}.

ATGA-DSC equipment (STA449F3 Jupiter; Netzsch, Selb, Germany) was used to determine the thermal stability of the films. For this purpose, the polymeric membrane was placed into an aluminum crucible, which was then placed in a TGA chamber. Subsequently, the sample was treated under a nitrogen flow and heated up from an ambient temperature to 600 °C at 10 °C·min^{-1}. The decomposition temperature of the polymers was determined in a TA Instruments Thermogravimetric Analyzer TGA5500 (TA Instruments, New Castle, DE, USA), using samples of around 10 mg, at a temperature range of 30 °C to 800 °C, in a nitrogen atmosphere and a heating rate of 10 °C·min^{-1}. A second-generation Bruker D2-Phaser diffractometer was employed to obtain the diffractograms corresponding to polymer films of 2 × 2 cm in size and around 400 μm in thickness. For this purpose, CuK_α radiation (1.54 Å) was used at 30 kV, 10 mA, and a 2θ scale from 7 to 70°. A Sartorius analytical balance model, Quintix 124-1 s, was used to determine the density of the membranes through the flotation method using ethanol as the liquid, in ambient conditions. The density measurements were repeated five times and the average of these values was reported for each sample.

Elemental distribution scanning, from the polymers in a membrane form, was performed by Scanning Electron Microscopy using JEOL IT300 equipment (JEOL, Tokyo, Japan). Atomic force microscopy was measured with a Bruker model Multimode 8, using the tapping mode of a Sharp Nitride Lever probe SNL-10 (Bruker, CA, USA). Membranes of 0.5 × 0.5 cm and around 400 μm in thickness were used for SEM and AFM analyses. The Cannon-Ubbelohde viscometer No. 50 was used to determine the inherent viscosity, η_{inh}, of the polymers. Dissolutions of 0.2 g of each polymer in 100 mL of DMSO were prepared at 30 °C. The η_{inh} measurements were repeated five times under the given conditions and the average of the values obtained for each polymer sample was reported.

The proton conductivity, σ_p, was determined from *EIS* measurements using a Swagelok cell with 2 current collectors and electrodes of SS 316 using a Biologic VSP potentiostat with FRA, model VMP3B-10, from 1 MHz to 1 Hz at a 50 mV amplitude and open circuit potential under 100% relative humidity at 30 °C; the values were obtained from a Nyquist plot. The mathematical expression used for calculating the proton conductivity is as follows:

$$\sigma_p = \frac{l_m}{10 \times A_T \times R_e} \quad (1)$$

where σ_p (mS·cm^{-1}) represents the proton conductivity, l_m is the membrane thickness (μm), A_T is the cross-section area of the membrane (cm^2), and R_e is the resistance value of the membrane obtained through the AC impedance method (Ω).

All characterizations were conducted in ambient conditions of humidity and temperature (55% RH and 25 °C, respectively) unless otherwise indicated.

2.2. Reagents

Comonomers: muconic acid (MUA), 4,4′-(hexafluoroisopropylidene)bis(*p*-phenylen eoxy)dianiline (HFDA), 2,5-diaminobencensulfonic acid (DABS), and 4,4′-Diamino-2,2′-stilbenedisulfonic acid (DASDA) were used as received. Calcium chloride ($CaCl_2$), 1-methyl-2-pyrrolidinone (NMP), triphenylphosphite (TPP), and pyridine (Py) were used in the polycondensation reaction without further purification. Finally, solvents dimethyl sulfoxide (DMSO), dimethylformamide (DMF), and methanol were used as received. All chemical reactants and solvents were acquired from Sigma-Aldrich, Inc. (St. Louis, MO, USA).

2.3. Synthesis of the Polyamides

A typical polymerization experiment was conducted as follows: an equimolar mixture of muconic acid and diamines were added to a 50 mL 3-neck flask equipped with a mechanical stirrer in a dry nitrogen atmosphere and according to the amounts shown in Table 1. Then, 2 mL of 1-methyl-2-pyrrolidinone (NMP) and 15 wt% calcium chloride ($CaCl_2$) were also added and continuously stirred for 5 min. Then, 0.41 mL of pyridine and 0.41 mL of triphenylphosphite (TPP) were added and maintained with moderate stirring until a fully incorporated mixture was achieved (see Schemes 1 and 2). Finally, the mixture was heated at 110 °C for 12 h and kept under a constant-stirring condition. Then, the reaction mixture was cooled to room temperature and then precipitated into methanol. The polymer obtained was washed repeatedly with hot water to be purified, and finally it was dried at 100 °C in a vacuum oven for 24 h.

Table 1. Molar relations of monomers in the feed for the synthesis of the muconic acid-based polyamide series.

Polymer	MUA [a] (mmol)	HFDA [b] (mmol)	DABS [c] (mmol)	DASDA [d] (mmol)
MUFA	0.64	0.64	0.00	0.00
MUFABA14	0.64	0.48	0.16	0.00
MUFABA24	0.64	0.32	0.32	0.00
MUFABA34	0.64	0.16	0.48	0.00
MUFASA14	0.64	0.48	0.00	0.16
MUFASA24	0.64	0.32	0.00	0.32
MUFASA34	0.64	0.16	0.00	0.48

[a] Muconic acid, [b] 4,4′-(hexafluoroisopropylidene)bis(*p*-phenyleneoxy)dianiline, [c] 2,5-diaminobencensulfonic acid, [d] 4,4′-Diamino-2,2′-stilbenedisulfonic acid.

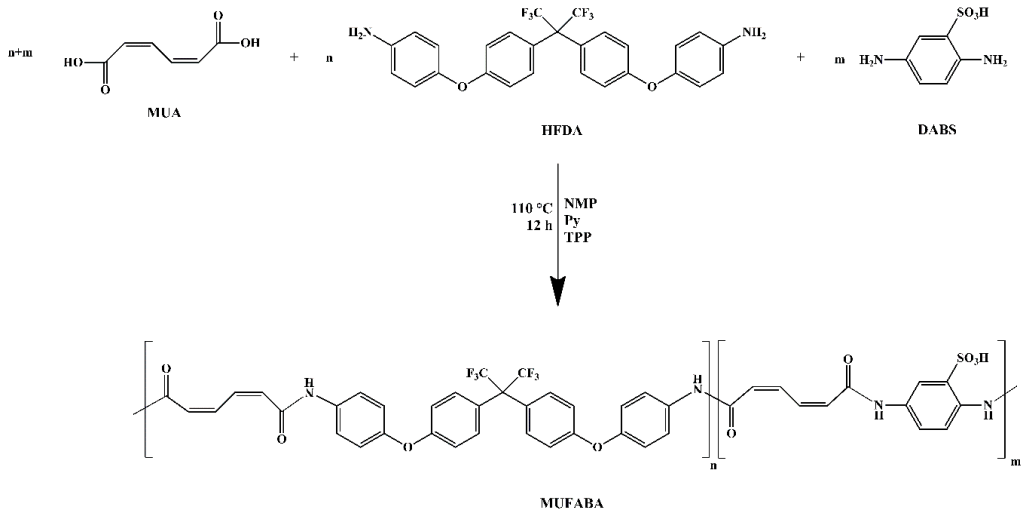

Scheme 1. Synthesis route of DABS-containing muconic acid-based polyamides.

2.3.1. Characterization of Polymer MUFA

^{1}H-*NMR* (400 MHz, DMSO-d_6, ppm): δ 10.39 (–NH–, 2H), 7.77–7.75 (aromatic, 4H), 7.34–7.32 (aromatic, 4H), 7.13–7.04 (8H), 6.78 (2H), 6.48–6.23 (2H).

^{19}F-*NMR* (376 MHz, DMSO-d_6, ppm): δ −65.9.

2.3.2. Characterization of Polymer MUFABA14

^{1}H-*NMR* (400 MHz, DMSO-d_6, ppm): δ 10.37 (–NH–, 8H), 8.36 (aromatic, 1H), 7.99 (aromatic, 2H), 7.77–7.75 (aromatic, 12H), 7.34–7.32 (aromatic, 12H), 7.13–7.04 (aromatic, 24H), 6.76 (8H), 6.48–6.22 (8H).

^{19}F-*NMR* (376 MHz, DMSO-d_6, ppm): δ −65.9.

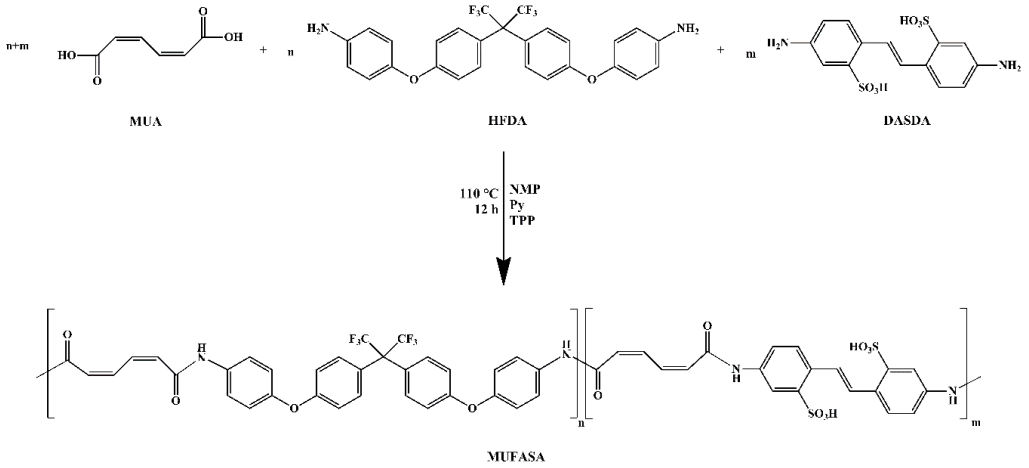

Scheme 2. Synthesis route of DASDA-containing muconic acid-based polyamides.

2.3.3. Characterization of Polymer MUFABA24

^{1}H-*NMR* (400 MHz, DMSO-d_6, ppm): δ 10.68–10.38 (–NH–, 8H), 8.39 (aromatic, 2H), 7.99 (aromatic, 4H), 7.77–7.75 (aromatic, 8H), 7.35–7.33 (aromatic, 8H), 7.14–7.05 (aromatic, 16H), 6.76 (8H), 6.49–6.23 (8H).

^{19}F-*NMR* (376 MHz, DMSO-d_6, ppm): δ −65.9.

2.3.4. Characterization of Polymer MUFABA34

^{1}H-*NMR* (400 MHz, DMSO-d_6, ppm): δ 10.68–10.38 (–NH–, 8H), 8.37 (aromatic, 3H), 8.03 (aromatic, 6H), 7.77 (aromatic, 4H), 7.35–7.33 (aromatic, 4H), 7.14–7.05 (8H), 6.76 (8H), 6.48–6.23 (8H).

^{19}F-*NMR* (376 MHz, DMSO-d_6, ppm): δ −65.9.

2.3.5. Characterization of Polymer MUFASA14

^{1}H-*NMR* (400 MHz, DMSO-d_6, ppm): δ 10.37 (–NH–, 8H), 8.09 (aromatic, 2H), 8.05 (aromatic, 2H), 7.77–7.75 (aromatic, 12H), 7.64 (aromatic, 2H), 7.46 (CH=CH, 2H), 7.34–7.32 (aromatic, 12H), 7.13–7.04 (aromatic, 24H), 6.76 (8H), 6.48–6.23 (8H).

^{19}F-*NMR* (376 MHz, DMSO-d_6, ppm): δ −65.9.

2.3.6. Characterization of Polymer MUFASA24

^{1}H-*NMR* (400 MHz, DMSO-d_6, ppm): δ 10.49–10.39 (–NH–, 8H), 8.11 (aromatic, 4H), 8.02 (aromatic, 4H), 7.76 (aromatic, 8H), 7.64 (aromatic, 4H), 7.46 (CH=CH, 4H), 7.34–7.32 (aromatic, 8H), 7.13–7.05 (aromatic, 16H), 6.74 (8H), 6.48–6.23 (8H).

^{19}F-*NMR* (376 MHz, DMSO-d_6, ppm): δ −65.9.

2.3.7. Characterization of Polymer MUFASA34

^{1}H-*NMR* (400 MHz, DMSO-d_6, ppm): δ 10.50–10.40 (–NH–, 8H), 8.11 (aromatic, 6H), 8.01 (aromatic, 6H), 7.77–7.75 (aromatic, 4H), 7.66–7.62 (aromatic, 6H), 7.45 (CH=CH, 6H), 7.34–7.32 (aromatic, 4H), 7.12–7.04 (8H), 6.76 (8H), 6.48–6.23 (8H).

^{19}F-*NMR* (376 MHz, DMSO-d_6, ppm): δ −65.9.

2.4. Membrane Preparation, Ion-Exchange Capacity, and Water Uptake

Membranes were cast from polymeric DMSO solutions at 60 °C. The solution was filtered and poured onto a glass plate, and the solvent was slowly evaporated in a controlled DMSO atmosphere. Then, the membranes were subjected to treatment as described in the literature [32]. This treatment consisted firstly in the removal of the residual solvent by using methanol and deionized water, followed by activation with 1.0 N of hydrochloric

acid. Finally, the membranes were dried under vacuum conditions at 150 °C for 24 h. The average thickness of the films was around 400 µm.

The experimental ion-exchange capacity of the polymer membrane was assessed, as described in the literature [32], by the titration method using the following mathematical expression:

$$IEC = \frac{V \times M}{W_{dry}} \quad (2)$$

where IEC (meq·g^{-1}) represents the ion-exchange capacity, V (mL) represents the volume of the NaOH solution used in the titration, M is the molarity of the solution, and W_{dry} (g) is the mass of the dried membrane.

The theoretical ion-exchange capacity was calculated considering the complete incorporation of monomers and according to the following mathematical expression:

$$IEC_{Theo} = \frac{n_{MS} \times 1000 \times sg}{w_{MUA} + w_{HFDA} + w_{MS}} \quad (3)$$

where IEC_{Theo} (meq·g^{-1}) represents the theoretical ion-exchange capacity, n_{MS} (mol) represents the moles of the sulfonated diamine present on the polymer, sg is the number of sulfonic groups corresponding to the DABS or DASDA sulfonated monomers, w_{MUA} (g) is the weight of monomer MUA, w_{HFDA} (g) is the weight of fluorinated monomer HFDA, and w_{MS} (g) is the weight of sulfonated monomers DABS or DASDA.

The water uptake, W_u, of the polymer membrane was estimated, as described in the literature [33], by gravimetric measurements employing the mathematical expression given below:

$$W_u = \frac{W_{wet} - W_{dry}}{W_{dry}} \times 100 \quad (4)$$

where W_u (%) represents the water uptake, W_{wet} (g) is the mass of the hydrated membrane, and W_{dry} (g) is the mass of the dried membrane.

3. Results and Discussion

Partially renewable muconic acid-based polyamides with an increasing degree of sulfonation were successfully prepared by a polycondensation reaction employing muconic acid as a renewable monomer and 4,4′-(hexafluoroisopropylidene)bis(*p*-phenyleneoxy)diani line (HFDA) as a fluorinated comonomer, as well as 2,5-diaminobencensulfonic acid (DABS) and 4,4′-diamino-2,2′-stilbenedisulfonic acid (DASDA) as sulfonated comonomers (see Schemes 1 and 2, respectively). The roles of DABS and DASDA in this study were to incorporate sulfonic acid groups into the polymer backbone, thus endowing the resulting polymer with proton-exchange properties suitable for being used as a PEM. In addition, the use of both diamines allowed us to elucidate the effect of the number of sulfonic acid groups per repeating unit on the overall property balance.

It could be seen that the degree of sulfonation, *DS*, was effectively adapted by adjusting the molar ratio of diamines fed at the beginning of the reaction. Images of the raw DABS- and DASDA-containing partially renewable polyamides synthesized in this study are presented in Figures 1 and 2, respectively. The non-sulfonated polyamide MUFA yielded yellow fibers and the sulfonated polyamide MUFABA series (Figure 1b–d) afforded fibers with coloration ranging from banana yellow to pineapple yellow, according to the increment in the sulfonation degree. In the same way, the sulfonated MUFASA series (Figure 2b–d) afforded fibers with coloration ranging from banana yellow to golden ochre. From these figures, it also can be seen that the raw material size decreases as the DS increases. According to the latter, the particle size is larger for the DABS-containing polyamides than for the MUFASA polyamides obtained from the same feed ratio. Polymeric membranes were prepared by casting and dissolving the polymers in DMSO. The membrane MUFA, Figure 1d, is transparent in appearance and quite resistant when touched; when the feed amount of sulfonated diamine increases in the polyamides, MUFABA or MUFASA series,

the membranes are opaque with an orange-brown color that progressively intensifies as the *DS* increases.

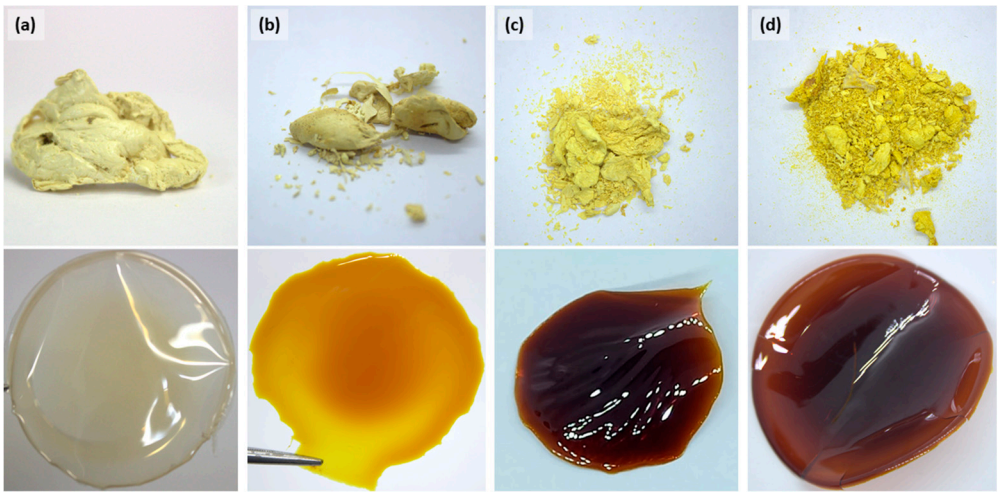

Figure 1. Photographic images of the synthesized raw muconic acid-based polyamides (**top**) and their corresponding polymeric membranes (**bottom**): (**a**) MUFA, (**b**) MUFABA14, (**c**) MUFABA24, and (**d**) MUFABA34.

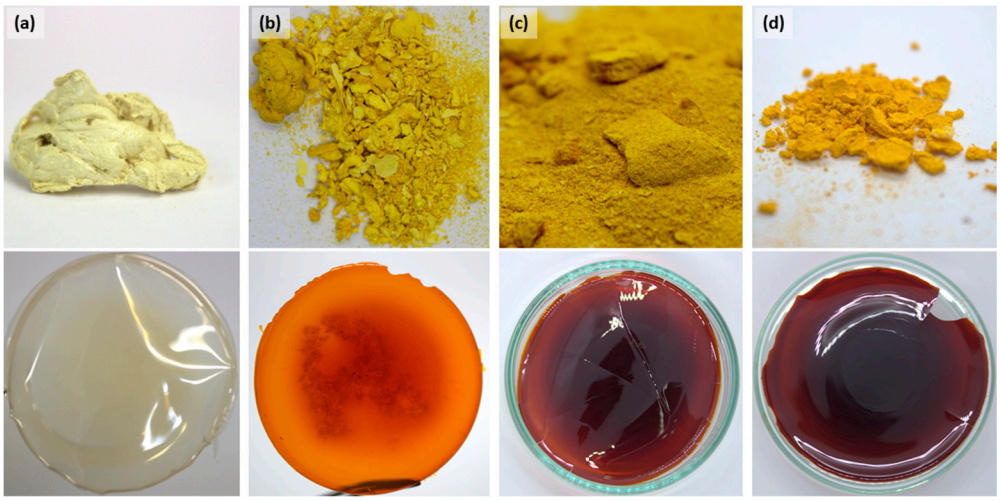

Figure 2. Photographic images of the synthesized raw muconic acid-based polyamides (**top**) and their corresponding polymeric membranes (**bottom**): (**a**) MUFA, (**b**) MUFASA14, (**c**) MUFASA24, and (**d**) MUFASA34.

The chemical structures of the new muconic acid-based polyamides were first confirmed by *FTIR* spectroscopy. The *FTIR* spectra of these new polyamides are shown in Figure 3; on the left side, the *FTIR* spectra of the series of polyamides containing DABS can be observed, while on the right side, those corresponding to the series of polyamides containing DASDA are shown. In both series, the characteristic absorption band for the N–H bond is observed at around 3300 cm^{-1}. The band associated with the amide carbonyl groups (–CONH–) is displayed close to 1660 cm^{-1}. The absorption band of C=C is exhibited at around 1500 cm^{-1}. The band attributed to the C–F bond can be observed at around 1200 cm^{-1}; this signal is more intense in the MUFA polymer, and it decreases as the concentration of the sulfonic acid increases. The presence of the sulfonic acid groups in the polymer backbone is indicated by the absorption bands shown at around 1086 and 1020 cm^{-1}, which correspond to the asymmetric and symmetric O=S=O stretching vibrations of the $–SO_3H$ groups. It should be noted that these signals increase as the concentration of these sulfonic groups increase. The signal observed at around 3400 cm^{-1}

can be attributed to the moisture present in the samples, which correlates with a higher concentration of sulfonic groups that makes these polymers more hydrophilic.

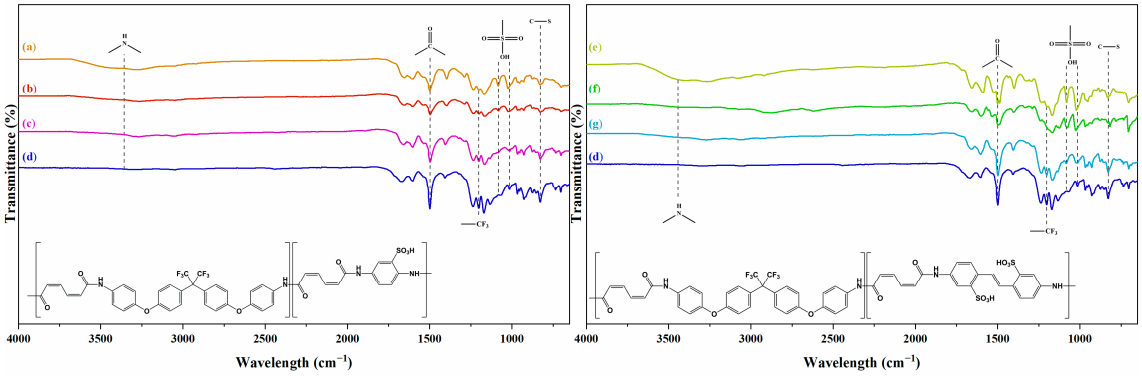

Figure 3. *FTIR* spectra of the muconic acid-based polyamides: (**Left**): (a) MUFABA34, (b) MUFABA24, (c) MUFABA14, (d) MUFA; (**Right**): (e) MUFASA34, (f) MUFASA24, (g) MUFASA14, and (d) MUFA.

NMR spectroscopy was performed to confirm the chemical structures and compositions of the novel muconic acid-based polyamides, thus corroborating the results obtain by *FTIR*. The ^{1}H-*NMR* spectra of the MUFABA and MUFASA polyamide series are shown in Figures 4 and 5, respectively. This analysis indicated that the ratio of the proton integration areas agreed quite well with the expected chemical structures of the polyamides. For instance, in Figure 4, a single signal ascribed to the proton attached to the amide group (H_c) in the polyamide MUFA can be observed at δ = 10.39 ppm. For the DABS-containing polyamide series, the proton attached to the amide group displays two signals, in $\delta \approx 10.68$ (H_g) and 10.38 ppm (H_c), and it can also be seen that the new signal at 10.68 ppm increases as the concentration of DABS in the polymer increases. Likewise, the signals observed in the region of 8.4–7.9 ppm are attributed to the aromatic protons in the DABS moiety (H_h, H_i, H_j). The signals attributed to the incorporation of the HFDA monomer appear at around $\delta \approx 7.7$ (H_f), 7.3 (H_d), and 7.11–7.04 ppm (H_e), while the olefinic proton signals ascribed to the incorporation of the muconic acid monomer (H_a, H_b) are observed at around 6.8–6.7 ppm; these monomer-derived signals are common for all polyamides synthesized in this study. Finally, in Figure 5, the DASDA-containing polyamide series presents multiple signals attributed to the proton attached to the amide group, in $\delta \approx 10.50$ (H_g, H_l) and 10.40 ppm (H_c). Moreover, the signals observed in the region of 8.1–7.6 ppm are attributed to the aromatic protons in the DASDA moiety (H_h, H_i, H_j, H_k).

The intensity of these signals varied progressively according to the fluorinated/sulfonated diamine feed molar ratio. The triplet peaks at around $\delta \approx 8.5$ ppm in the ^{1}H-*NMR* spectra were attributed to pyridine, a reactive used in the synthesis of these polyamides, which was not completely removed after the purification procedure. The ratio between the proton integration areas that remained unchanged in the polyamide MUFA and the series of sulfonated polyamides, MUFABA and MUFASA, were employed to calculate the *DS*. The values of *DS*, determined from the ^{1}H-*NMR* spectra, for the muconic acid-based polyamides MUFABA14; MUFABA24; and MUFABA34 were found to be 24.3%; 48.7%; and 72.2%, respectively, while those of the polyamides MUFASA14; MUFASA24; and MUFASA34 were found to be 22.8%; 46.1%; and 70.6%, respectively. These *DS* values were close and could be correlated to the diamine ratio established in the feed values (HFDA, and DABS or DASDA) of the new polyamides, which were 25%, 50%, and 75% with respect to the sulfonated diamine, for each series, respectively (see Table 1). These values indicated that the incorporation of sulfonic groups was effectively controlled.

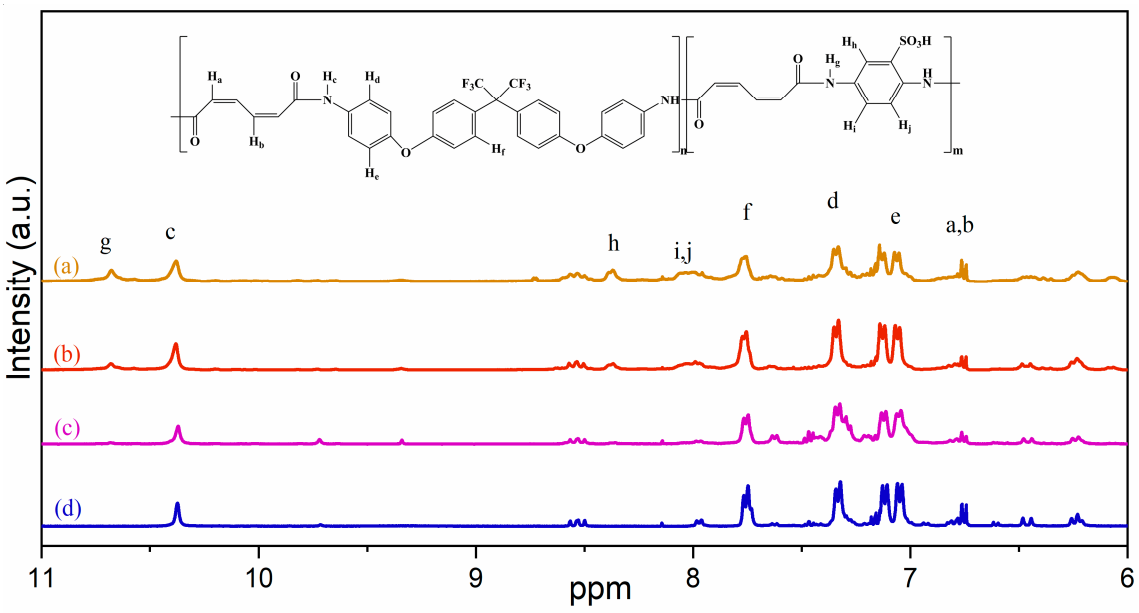

Figure 4. ^{1}H-*NMR* spectra of the muconic acid-based polyamides: (a) MUFABA14, (b) MUFABA24, (c) MUFABA34, and (d) MUFA. Lower case letters correspond to the protons indicated in the chemical structure.

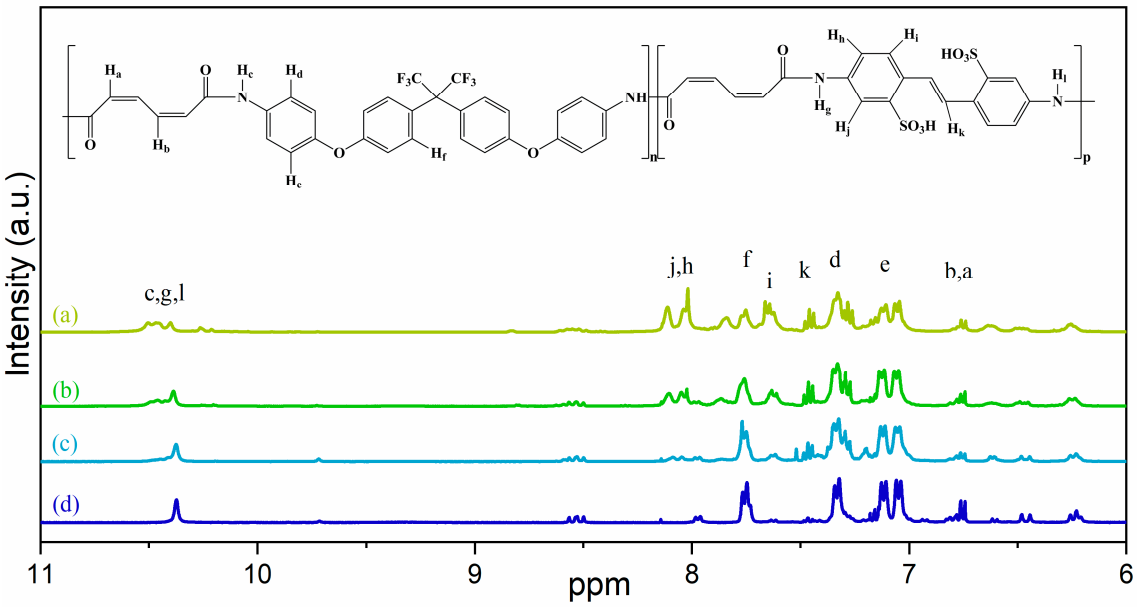

Figure 5. ^{1}H-*NMR* spectra of the muconic acid-based polyamides: (a) MUFASA34, (b) MUFASA24, (c) MUFASA14, and (d) MUFA. Lower case letters correspond to the protons indicated in the chemical structure.

The T_g of the polymers was determined by *DSC*, and their thermograms are shown in Figure 6; those corresponding to the DABS-containing polyamide series are displayed on the left side, while those corresponding to the DASDA-containing polyamide series are shown on the right. The DSC curves present some features lower than 200 °C; those observed around 100 °C are attributed to the humidity adsorbed by the membranes, while those observed near 200 °C are attributed to the residual solvent (DMSO) used in the membrane casting. Therefore, the glass transition temperature of the polymer was considered to be the first characteristic above 200 °C. It can be seen that the T_g for the non-sulfonated polymer MUFA is about 241 °C, a high T_g that is ascribed to the rigidity of the main chain caused by the aromatic rings of the HFDA monomer. It was found that for the MUFABA series, the T_g

remained almost the same. The T_g values for MUFABA14, MUFABA24, and MUFABA34 were found to be 244 °C, 240 °C, and 241 °C, respectively. The latter can be attributed to two opposite effects. On the one hand, as DS increases, the ratio of fluorinated/sulfonated diamine decreases, and, in turn, so does the rigidity of the polymer chains. On the other hand, the incorporation of sulfonic acid groups creates strong ionic interactions between polymeric chains, increasing their rigidity. This contrasting behavior results in a negligible change in T_g as the quantity of the sulfonated moiety is varied in the polymer. It was also found that for the MUFASA series, the T_g increased as the *DS* increased. The T_g values for MUFASA14, MUFASA24, and MUFASA34 were found to be 217 °C, 229 °C, and 232 °C, respectively. This increase in the T_g value of the MUFASA series could be due to the higher concentration of sulfonic groups in the polymer backbone, which inhibited the relaxation process of polymer main chains as a result of strong ionic interactions between them.

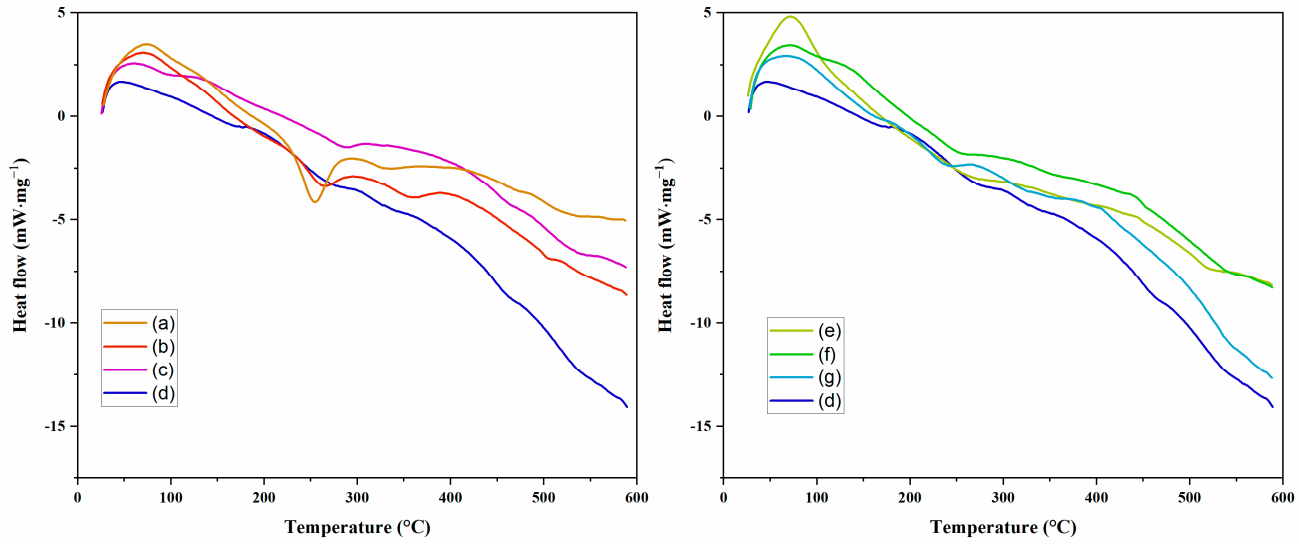

Figure 6. *DSC* thermograms of the DABS-containing polyamide series (**left**): (a) MUFABA34, (b) MUFABA24, (c) MUFABA14, and (d) MUFA, and the DASDA-containing polyamide series (**right**): (e) MUFASA34, (f) MUFASA24, (g) MUFASA14, and (d) MUFA.

The thermal stability of polyamides was studied by *TGA* under a nitrogen atmosphere. The thermograms are presented in Figure 7 with a 2% offset between each thermogram. It can be observed that the polymer MUFA exhibits a decomposition temperature, T_d, of about 322 °C. For the MUFABA series, the T_d values observed were 318 °C, 303 °C, and 273 °C for MUFABA14, MUFABA24, and MUFABA34, respectively, while for the MUFASA series, the T_d values observed were 287 °C, 272 °C, and 276 °C for MUFASA14, MUFASA24, and MUFASA34, respectively. From these results, it is clear that the introduction of labile groups, such as $-SO_3H$, into the macromolecular architecture is reflected by a lower T_d value.

The mean intersegmental distance or *d-spacing* between the polymer chains was calculated by the Bragg's equation, $d_i = \frac{n\lambda}{2sin(\theta)}$; the angle was determined at the maximum intensity of the amorphous peak. In general, the *XRD* technique showed patterns characteristic of amorphous polymeric materials, and the absences of narrow peaks showed that these samples did not exhibit any degree of crystallinity, with the exception of the MUFASA34 sample, in which the highest quantity of the DASDA monomer incorporated seemed to induce a certain degree of crystallinity in the resulting polymer (see Figure 8). The maximum reflective intensity was observed at interval of $2\theta \approx 17.5–24.6°$. This angle increased as the degree of sulfonation increased.

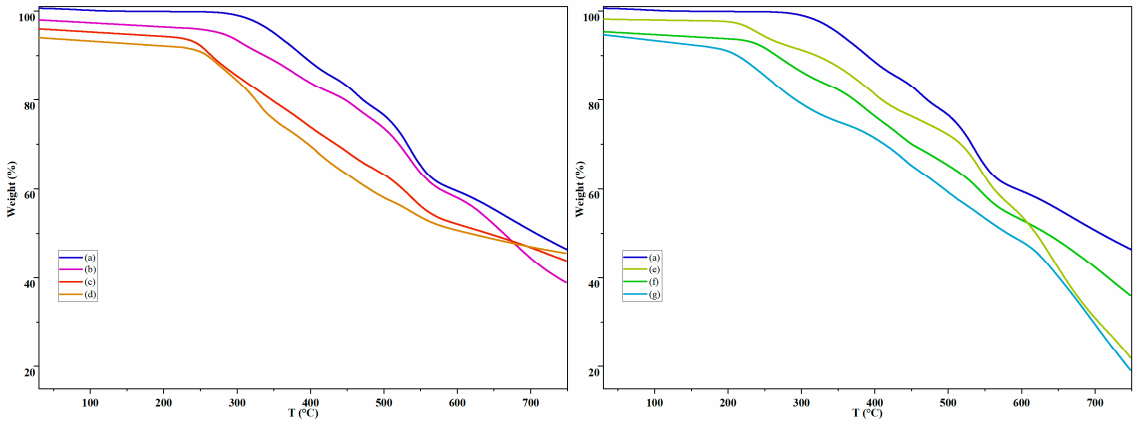

Figure 7. *TGA* thermograms of the DABS-containing polyamide series (**left**): (a) MUFA, (b) MUFABA14, (c) MUFABA24, and (d) MUFABA34, and the DASDA-containing polyamide series (**right**): (a) MUFA, (e) MUFASA14, (f) MUFASA24, and (g) MUFASA34.

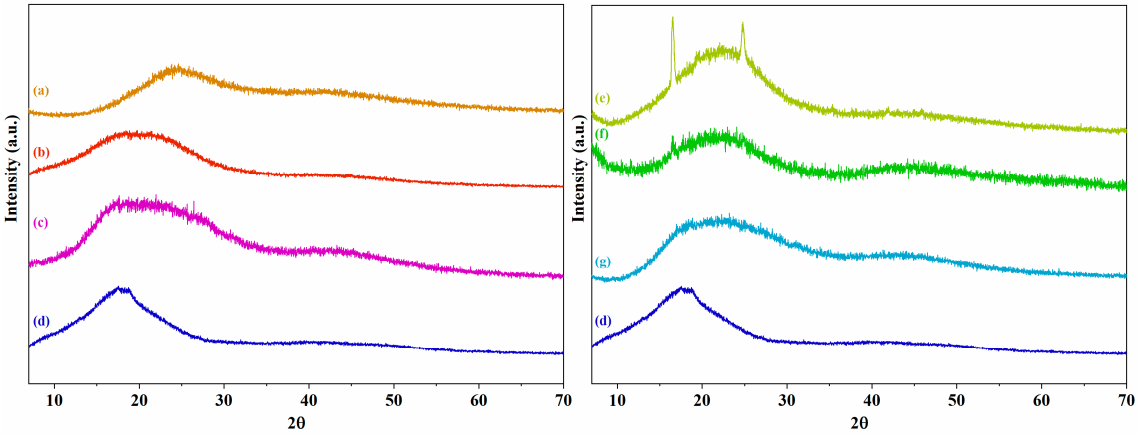

Figure 8. *XRD* patterns of the DABS-containing polyamide series (**left**): (a) MUFABA34, (b) MUFABA24, (c) MUFABA14, and (d) MUFA, and the DASDA-containing polyamide series (**right**): (e) MUFASA34, (f) MUFASA24, (g) MUFASA14, and (d) MUFA.

The density, ρ, of the new polyamide membranes was determined by the flotation method using ethanol as the liquid, at room temperature. The values, shown in Table 2, were found to range from 1.38 to 1.45 g·cm^{-3}. The inherent viscosity (η_{inh}), also shown in Table 2, presents values ranging from 0.352 to 0.201 dL·g^{-1}. It can be seen that the lowest inherent viscosity is that of the MUFASA34 polymer, indicating that the chain size of this polymer is smaller than that of the other polymers. The η_{inh} values obtained are in the range of other synthetic polymers [34,35]. The η_{inh} values of the DABS-containing polyamides are very similar to each other, whereas the η_{inh} values of the DASDA-containing polyamides decrease as the *DS* increases; it is likely that the higher amount of DASDA in the feed causes the insolubility of the reactants in the polymer solution, affecting the growth of the polymer.

The morphology of the membranes was observed by *AFM* and the topographic images obtained by this technique, in tapping mode, are presented in Figure 9. The morphology of the MUFABA14 sample is mainly characterized by voids and a few areas with protuberances that can be associated with hydrophobic fluorine-rich regions. The MUFABA24 sample presents a homogeneous surface morphology, in which the existence of voids or large protuberances is not appreciated; this can be attributed to the balance between the hydrophobic and hydrophilic regions created by the sulfonic acid groups. In contrast, the MUFABA34 sample shows a quite irregular surface morphology consisting of plateaus immersed in regions with protuberances of different sizes that can be attributed to the

higher number of $-SO_3H$ groups in this entire series of polyamides, which causes the disruption of the chain-packing process. The topology of MUFASA14 is mainly characterized by a regular surface formed by small protuberances that lacks voids and resembles that of MUFABA14. The MUFASA24 sample exhibits a surface morphology that is composed of different plateaus and some areas with pinnacles in which phase segregation can be noticed. Finally, the MUFASA34 sample shows a surface on which quite large protuberances can be seen. Due to the high *DS* of this polyamide, it is likely that large hydrophilic regions are formed and these begin to segregate from the hydrophobic regions, giving rise to large clusters. These observations indicate the existence of phase separation, which is a fundamental aspect to achieve high proton conductivity, since the segregation of hydrophilic and hydrophobic phases builds the channels through which ionic transport is conducted.

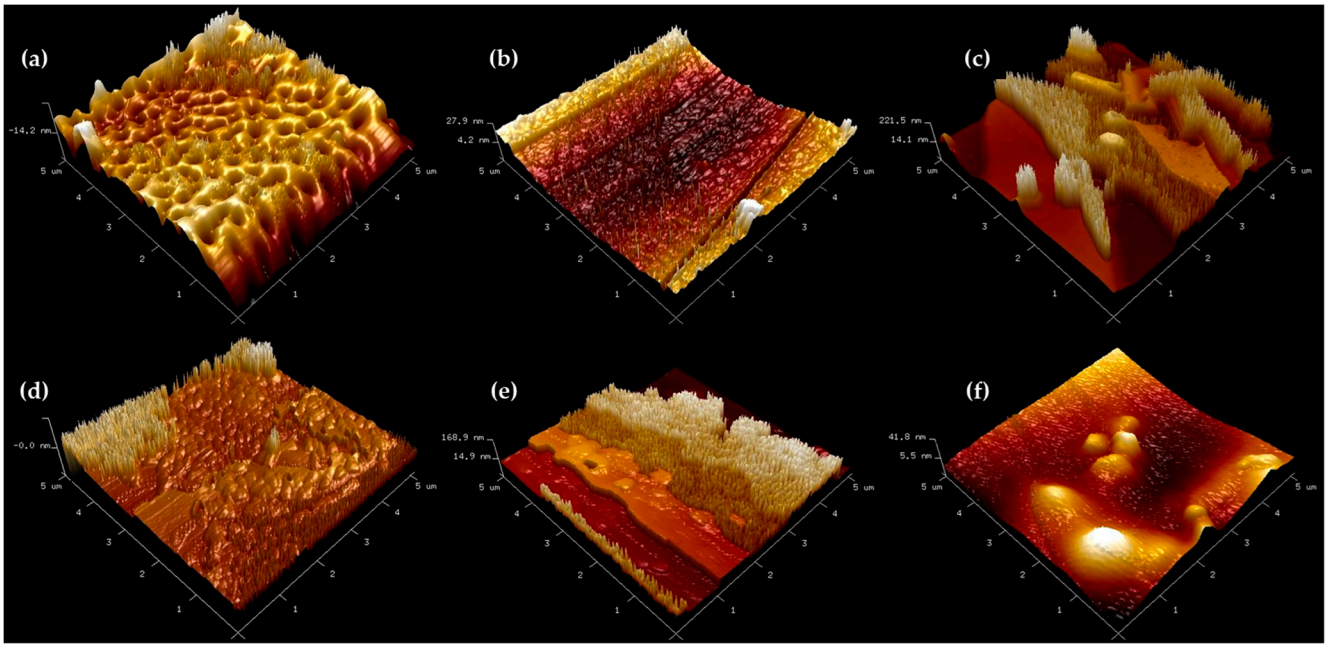

Figure 9. Three-dimensional *AFM* micrographs (5 × 5 μm) of (**a**) MUFABA14, (**b**) MUFABA24, (**c**) MUFABA34, (**d**) MUFASA14, (**e**) MUFASA24, and (**f**) MUFASA34.

Table 2. Physical properties of the muconic acid-based polyamide series.

Polymer	T_g (°C) [a]	T_d (°C) [b]	d_i (Å) [c]	ρ (g·cm^{-3}) [d]	η_{inh} (dL·g^{-1}) [e]
MUFA	241	322	2.55	1.38	0.352
MUFABA14	244	318	2.05	1.38	0.343
MUFABA24	240	303	2.27	1.39	0.304
MUFABA34	241	273	1.85	1.43	0.348
MUFASA14	217	287	1.95	1.37	0.266
MUFASA24	229	272	1.97	1.38	0.213
MUFASA34	232	276	2.05	1.45	0.201

[a] Glass transition temperature determined by *DSC*. [b] Decomposition temperature determined by *TGA*. [c] Average separation distance between polymer chains determined by *XRD*. [d] Density determined by the flotation method. [e] Inherent viscosity at a polymer concentration of 0.2 g·dL^{-1}.

Scanning electron microscopy (*SEM*) and energy-dispersive X-ray spectroscopy (*EDS*) were employed to study the surfaces of the polyamide samples with the highest content of sulfonic acid groups in each series. Representative results are shown in Figures 10 and 11, corresponding to polymers MUFABA34 and MUFASA34, respectively. The *SEM* images show the heterogeneous surface texture and morphology for these partially renewable ionomers that can be attributed to phase segregation. Furthermore, *EDS* was employed

to estimate the chemical composition of the polymers. As can be seen, both polyamide samples mainly show the presence of carbon (C), oxygen (O), sulfur (S), fluorine (F), nitrogen (N), and calcium (Ca). These results, specifically the sulfur weight percent and fluorine weight percent determined by *EDS*, are in agreement with those expected from the fluorinated/sulfonated diamine feed molar ratio.

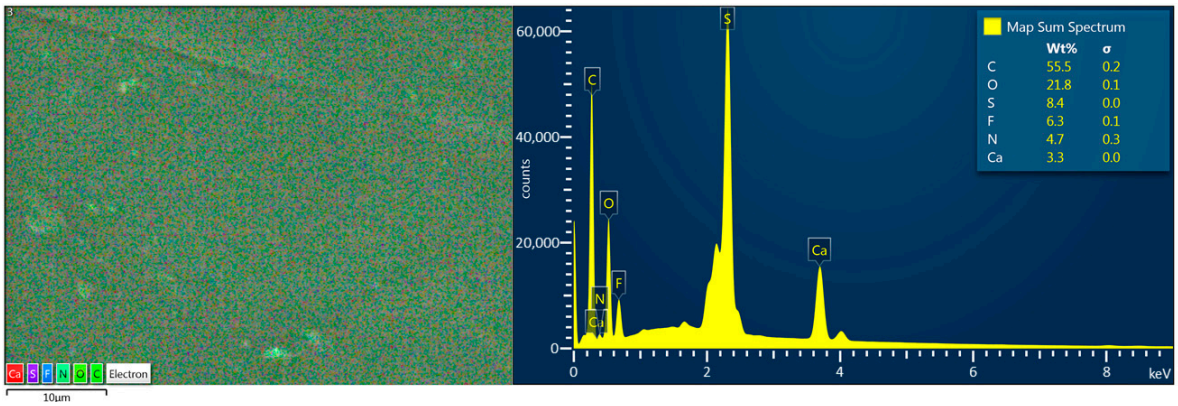

Figure 10. *SEM* image and *EDS* spectra of MUFABA34.

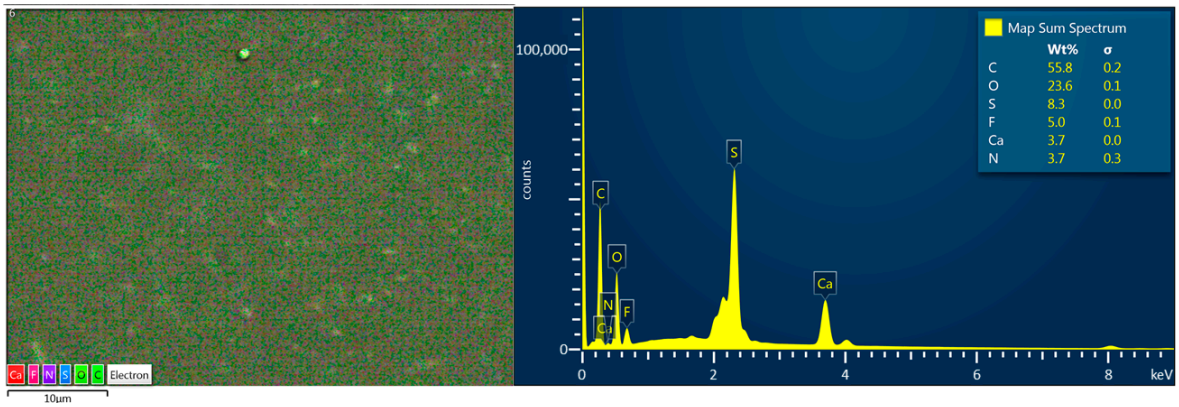

Figure 11. *SEM* image and *EDS* spectra of MUFASA34.

The electrochemical impedance spectroscopy (*EIS*) measurements of the sulfonated membranes were performed under 100% relative humidity at 30 °C in the range of 1 MHz to 1 Hz; Nyquist plots of the most sulfonated membranes of each series, MUFABA34 and MUFASA34, are shown in Figure 12. The resistance, R_e, of the membranes was calculated using the "ZFit" function of EC-Lab software V11.27 from the intersection with the abscissa axis, which corresponds to the resistance value, as can be observed in the insets of Figure 12; all measures are repeated three times in the given conditions, and the averages of the results obtained are reported. Then, the proton conductivity, σ_p, was calculated by Equation (1), and the results are presented in Table 3. It can be observed that the σ_p value increases as the sulfonic acid group concentration increases. The σ_p values for the MUFABA polyamide series were found to range from 0.027 to 1.608 mS·cm^{-1}, while those of the MUFASA polyamide series were found to range from 0.367 to 9.895 mS·cm^{-1}. It is important to mention that, when comparing a polyamide from the MUFABA series with one from the MUFASA series with similar *DS* values, the latter actually contains twice as many –SO_3H groups as the former, because the diamine DASDA, which gives rise to the MUFASA series, contains one more –SO_3H group than the diamine DABS, which gives rise to the MUFABA series. For this reason, the MUFASA34 membrane, with a DS = 70.6%, shows higher *IEC* and σ_p values than the MUFABA34 membrane that shows a DS = 72.2%. The polyamide MUFASA34 is the one that contains the highest number of sulfonic acid groups of both series of new polyamides. Due to the latter reason, it also shows the highest *IEC* and W_u

values, which in turn is reflected in the highest proton conductivity of all the materials synthesized in this study.

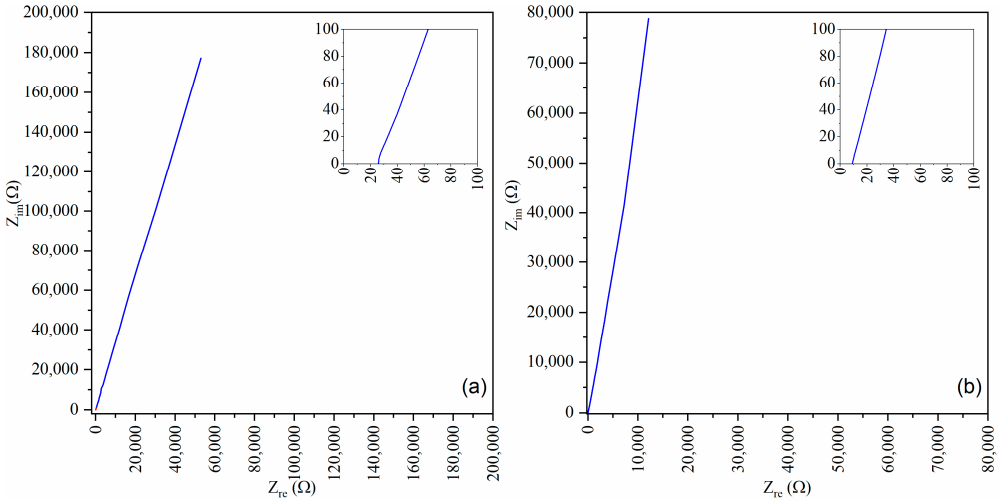

Figure 12. Nyquist plots of (**a**) MUFABA34 and (**b**) MUFASA34. Inset: zoomed-in view of the Nyquist plots in the high-frequency-region membrane.

Table 3. Ionic properties of novel muconic acid-based polyamides.

Polymer	*DS* [a] (%)	*IEC* (mmol·g^{-1}) Theoretical	*IEC* (mmol·g^{-1}) Experimental [b]	W_u (%)	σ_p (mS·cm^{-1}) [c]
MUFA	-	-	-	4.51	-
MUFABA14	24.3	0.43	0.37	7.87	0.027
MUFABA24	48.7	1.01	0.96	29.17	0.426
MUFABA34	72.2	1.82	1.80	33.49	1.608
MUFASA14	22.8	0.80	0.72	12.45	0.367
MUFASA24	46.1	1.70	1.80	28.78	0.849
MUFASA34	70.6	2.73	2.81	36.93	9.895

[a] Determinated by ^{1}H-*NMR*. [b] Determined by titration. [c] Determinated by *EIS*.

Various efforts have been made to develop sulfonated polymeric materials with a sustainable approach around the world [36–40]. Table 4 shows some of these materials, along with their ionic properties, and compares them with the values obtained for the muconic acid-based polymers developed in this research. The results obtained for the sulfonated polymers MUFABA34 and MUFASA34 are comparable with other fully or partially renewable polymers bearing sulfonic acid groups. The latter indicates that the sustainable methodology addressed in this study is an effective tool to offer special environmentally friendly polymers.

Table 4. Ionic properties' comparison of the muconic acid-based ionomers reported in this study and some renewable polymers reported in the literature.

Polymer	IEC_{Exp} (meq·g^{-1}) [a]	W_u (%) [b]	σ_p (mS·cm) [c]	Reference Author
(SPEAE) [d]	0.356	51.2	0.018	[36]
S5 [e]	-	-	0.005	[37]
DASA [f]	2.2	44.1	0.5	[38]
CH [g]	0.37	249	2.44	[39]
DAFASA2/4 [f]	0.8	17.1	1.5	[38]
LS 1.6 [h]	1.6	25.9	8.12	[40]

Table 4. *Cont.*

Polymer	IEC_{Exp} (meq·g^{-1}) [a]	W_u (%) [b]	σ_p (mS·cm) [c]	Reference Author
MUFABA34	1.80	33.49	1.608	This study
MUFASA34	2.81	36.93	9.895	This study

[a] Ion-exchange capacity determined by titration. [b] Water uptake determined by gravimetric measurements. [c] Proton conductivity determined by *EIS*. [d] Sulfonated poly(eugenolco-allyleugenol). [e] Chitosan-based membranes containing acetic acid (HAC) and plasticized with glycerol. [f] Oleic acid-based polyamide. [g] Pristine chitosan. [h] Ionomer from kraft lignin.

4. Conclusions

The muconic acid monomer reacted successfully in polycondensation reactions with two aromatic-sulfonated diamines and a fluorinated diamine as comonomers for the synthesis of two series of partially renewable aromatic–aliphatic polyamides with an increasing degree of sulfonation (*DS*). *FTIR* and *NMR* spectroscopy methods were employed to confirm the polymer chemical structures and also revealed that the *DS* was effectively tailored by adjusting the feed molar ratio of the diamines. It was also found that the W_u, *IEC*, and σ_p values increased together with the DS. The highest value of σ_p determined by electrochemical impedance spectroscopy (*EIS*) was found to be 9.895 mS·cm^{-1} at 30 °C corresponding to the MUFASA34 polyamide. The ionic properties reported in this study for the partially renewable muconic acid-based ionomers were close to other fully or partially renewable sulfonated polymers. It is important to note that the incorporation of renewable monomers is a powerful tool to synthesize sustainable and eco-friendly specialty polymers that can be an alternative for PEM applications.

Author Contributions: Conceptualization, A.A.S. and J.V.; data curation, C.C.-G., S.R.V.-G. and A.A.S.; investigation, C.C.-G. and A.O.; methodology, C.C.-G., T.E.S. and D.E.P.-C.; writing—original draft, C.C.-G. and J.V.; writing—review and editing, C.C.-G. and J.V. All authors have read and agreed to the published version of the manuscript.

Funding: Financial support from DGAPA-UNAM PAPIIT through project IN108022 is gratefully acknowledged.

Data Availability Statement: The data presented in this study are available from the corresponding authors upon reasonable request.

Acknowledgments: We are grateful to Gerardo Cedillo Valverde, Karla Eriseth Reyes Morales, M.C. José Martín Baas López, and M.C. Enrique Escobedo Hernández for their assistance in the *NMR*, thermal properties, *EIS*, and *AFM* experiments, respectively. Financial support from the National Council for Science and Technology of Mexico (CONACyT) (PhD Scholarship given to C.C-G.; number 762228) is gratefully acknowledged.

Conflicts of Interest: The authors declare no conflict of interest.

References

1. Park, M.; Hong, S.-J.; Kim, N.-K.; Shin, J.; Kim, Y.-W. Vegetable Oil-Derived Polyamide Multiblock Copolymers toward Chemically Recyclable Pressure-Sensitive Adhesives. *ACS Sustain. Chem. Eng.* **2023**, *11*, 10095–10107. [CrossRef]
2. Bottega Pergher, B.; Girigan, N.; Vlasblom, S.; Weinland, D.H.; Wang, B.; van Putten, R.-J.; Gruter, G.-J.M. Reactive Phenolic Solvents Applied to the Synthesis of Renewable Aromatic Polyesters with High Isosorbide Content. *Polym. Chem.* **2023**, *14*, 3225–3238. [CrossRef]
3. Mu, T.; Leng, S.; Tang, W.; Shi, N.; Wang, G.; Yang, J. High-Performance and Low-Cost Membranes Based on Poly(Vinylpyrrolidone) and Cardo-Poly(Etherketone) Blends for Vanadium Redox Flow Battery Applications. *Batteries* **2022**, *8*, 230. [CrossRef]
4. Mukoma, P.; Jooste, B.R.; Vosloo, H.C.M. Synthesis and Characterization of Cross-Linked Chitosan Membranes for Application as Alternative Proton Exchange Membrane Materials in Fuel Cells. *J. Power Sources* **2004**, *136*, 16–23. [CrossRef]
5. Li, N.; Shin, D.W.; Hwang, D.S.; Lee, Y.M.; Guiver, M.D. Polymer Electrolyte Membranes Derived from New Sulfone Monomers with Pendent Sulfonic Acid Groups. *Macromolecules* **2010**, *43*, 9810–9820. [CrossRef]
6. Li, J.; Pan, M.; Tang, H. Understanding Short-Side-Chain Perfluorinated Sulfonic Acid and Its Application for High Temperature Polymer Electrolyte Membrane Fuel Cells. *RSC Adv.* **2014**, *4*, 3944–3965. [CrossRef]

7. Iulianelli, A.; Clarizia, G.; Gugliuzza, A.; Ebrasu, D.; Bevilacqua, A.; Trotta, F.; Basile, A. Sulfonation of PEEK-WC Polymer via Chloro-Sulfonic Acid for Potential PEM Fuel Cell Applications. *Int. J. Hydrogen Energy* **2010**, *35*, 12688–12695. [CrossRef]
8. Ahmad, M.I.; Zaidi, S.M.J.; Rahman, S.U. Proton Conductivity and Characterization of Novel Composite Membranes for Medium-Temperature Fuel Cells. *Desalination* **2006**, *193*, 387–397. [CrossRef]
9. Xing, P.; Robertson, G.P.; Guiver, M.D.; Mikhailenko, S.D.; Wang, K.; Kaliaguine, S. Synthesis and Characterization of Sulfonated Poly(Ether Ether Ketone) for Proton Exchange Membranes. *J. Memb. Sci.* **2004**, *229*, 95–106. [CrossRef]
10. Devrim, Y.; Erkan, S.; Baç, N.; Eroğlu, I. Preparation and Characterization of Sulfonated Polysulfone/Titanium Dioxide Composite Membranes for Proton Exchange Membrane Fuel Cells. *Int. J. Hydrogen Energy* **2009**, *34*, 3467–3475. [CrossRef]
11. Santiago, A.A.; Vargas, J.; Fomine, S.; Gaviño, R.; Tlenkopatchev, M.A. Polynorbornene with Pentafluorophenyl Imide Side Chain Groups: Synthesis and Sulfonation. *J. Polym. Sci. Part A Polym. Chem.* **2010**, *48*, 2925–2933. [CrossRef]
12. Zhang, Z.; Liu, H.; Dong, T.; Deng, Y.; Li, Y.; Lu, C.; Jia, W.; Meng, Z.; Zhou, M.; Tang, H. Phosphonate Poly(Vinylbenzyl Chloride)-Modified Sulfonated Poly(Aryl Ether Nitrile) for Blend Proton Exchange Membranes: Enhanced Mechanical and Electrochemical Properties. *Polymers* **2023**, *15*, 3203. [CrossRef]
13. Zavorotnaya, U.M.; Ponomarev, I.I.; Volkova, Y.A.; Sinitsyn, V.V. Development of High-Performance Hydrogen-Air Fuel Cell with Flourine-Free Sulfonated Co-Polynaphthoyleneimide Membrane. *Membranes* **2023**, *13*, 485. [CrossRef] [PubMed]
14. Kim, A.R.; Poudel, M.B.; Chu, J.Y.; Vinothkannan, M.; Santhosh Kumar, R.; Logeshwaran, N.; Park, B.H.; Han, M.K.; Yoo, D.J. Advanced Performance and Ultra-High, Long-Term Durability of Acid-Base Blended Membranes over 900 Hours Containing Sulfonated PEEK and Quaternized Poly(Arylene Ether Sulfone) in H_2/O_2 Fuel Cells. *Compos. Part B Eng.* **2023**, *254*, 110558. [CrossRef]
15. Jiang, J.; Xiao, M.; Huang, S.; Han, D.; Wang, S.; Meng, Y. Phosphonic Acid-Imidazolium Containing Polymer Ionomeric Membranes Derived from Poly (Phenylene Oxide) towards Boosting the Performance of HT-PEM Fuel Cells. *J. Memb. Sci.* **2023**, *686*, 121982. [CrossRef]
16. Li, G.; Shen, R.; Hu, S.; Wang, B.; Algadi, H.; Wang, C. Norbornene-Based Acid–Base Blended Polymer Membranes with Low Ion Exchange Capacity for Proton Exchange Membrane Fuel Cell. *Adv. Compos. Hybrid Mater.* **2022**, *5*, 2131–2137. [CrossRef]
17. Woroch, C.P.; Cox, I.W.; Kanan, M.W. A Semicrystalline Furanic Polyamide Made from Renewable Feedstocks. *J. Am. Chem. Soc.* **2023**, *145*, 697–705. [CrossRef]
18. Reinaldo, J.S.; Milfont, C.H.R.; Gomes, F.P.C.; Mattos, A.L.A.; Medeiros, F.G.M.; Lopes, P.F.N.; Filho, M.d.S.M.S.; Matsui, K.N.; Ito, E.N. Influence of Grape and Acerola Residues on the Antioxidant, Physicochemical and Mechanical Properties of Cassava Starch Biocomposites. *Polym. Test.* **2021**, *93*, 107015. [CrossRef]
19. Zarna, C.; Opedal, M.T.; Echtermeyer, A.T.; Chinga-Carrasco, G. Reinforcement Ability of Lignocellulosic Components in Biocomposites and Their 3D Printed Applications–A Review. *Compos. Part C Open Access* **2021**, *6*, 100171. [CrossRef]
20. Terroba-Delicado, E.; Fiori, S.; Gomez-Caturla, J.; Montanes, N.; Sanchez-Nacher, L.; Torres-Giner, S. Valorization of Liquor Waste Derived Spent Coffee Grains for the Development of Injection-Molded Polylactide Pieces of Interest as Disposable Food Packaging and Serving Materials. *Foods* **2022**, *11*, 1162. [CrossRef] [PubMed]
21. Borrero-l, A.M.; Valencia, C.; Franco, J.M. Lignocellulosic Materials for the Production of Biofuels, Biochemicals and Biomaterials and Applications Of. *Polymers* **2022**, *14*, 881. [CrossRef]
22. Wolff, S.; Rüppel, A.; Rida, H.A.; Heim, H.-P. Emission and Mechanical Properties of Glass and Cellulose Fiber Reinforced Bio-Polyamide Composites. *Polymers* **2023**, *15*, 2603. [CrossRef]
23. Beppu, S.; Tachibana, Y.; Kasuya, K.I. Recyclable Polycarbosilane from a Biomass-Derived Bifuran-Based Monomer. *ACS Macro Lett.* **2023**, *12*, 536–542. [CrossRef]
24. Khalil, I.; Quintens, G.; Junkers, T.; Dusselier, M. Muconic Acid Isomers as Platform Chemicals and Monomers in the Biobased Economy. *Green Chem.* **2020**, *22*, 1517–1541. [CrossRef]
25. Quintens, G.; Vrijsen, J.H.; Adriaensens, P.; Vanderzande, D.; Junkers, T. Muconic Acid Esters as Bio-Based Acrylate Mimics. *Polym. Chem.* **2019**, *10*, 5555–5563. [CrossRef]
26. Liu, P.; Zheng, Y.; Yuan, Y.; Zhang, T.; Su, T.; Li, Q.; Liang, Q.; Qi, Q. A Circular Bioprocess for the Sustainable Conversion of Polyethylene Terephthalate to Muconic Acid with an Engineered Pseudomonas Putida. *SSRN Electron. J.* **2022**. [CrossRef]
27. Molinari, F.; Pollegioni, L.; Rosini, E. Whole-Cell Bioconversion of Renewable Biomasses-Related Aromatics to Cis,Cis-Muconic Acid. *ACS Sustain. Chem. Eng.* **2023**, *11*, 2476–2485. [CrossRef]
28. Nandhini, R.; Sivaprakash, B.; Rajamohan, N.; Vo, D.V.N. Lignin and Polylactic Acid for the Production of Bioplastics and Valuable Chemicals. *Environ. Chem. Lett.* **2022**, *21*, 403–427. [CrossRef]
29. Weiland, F.; Barton, N.; Kohlstedt, M.; Becker, J.; Wittmann, C. Systems Metabolic Engineering Upgrades Corynebacterium Glutamicum to High-Efficiency Cis, Cis-Muconic Acid Production from Lignin-Based Aromatics. *Metab. Eng.* **2023**, *75*, 153–169. [CrossRef] [PubMed]
30. Maniar, D.; Fodor, C.; Karno Adi, I.; Woortman, A.J.J.; van Dijken, J.; Loos, K. Enzymatic Synthesis of Muconic Acid-Based Polymers: Trans, Trans-Dimethyl Muconate and Trans, β-Dimethyl Hydromuconate. *Polymers* **2021**, *13*, 2498. [CrossRef] [PubMed]
31. Yan, K.; Wang, J.; Wang, Z.; Yuan, L. Bio-Based Monomers for Amide-Containing Sustainable Polymers. *Chem. Commun.* **2023**, *59*, 382–400. [CrossRef]

32. Santiago, A.A.; Ibarra-Palos, A.; Cruz-Morales, J.A.; Sierra, J.M.; Abatal, M.; Alfonso, I.; Vargas, J. Synthesis, Characterization, and Heavy Metal Adsorption Properties of Sulfonated Aromatic Polyamides. *High Perform. Polym.* **2018**, *30*, 591–601. [CrossRef]
33. Ruiz, I.; Corona-García, C.; Santiago, A.A.; Abatal, M.; Téllez Arias, M.G.; Alfonso, I.; Vargas, J. Synthesis, Characterization, and Assessment of Novel Sulfonated Polynorbornene Dicarboximides as Adsorbents for the Removal of Heavy Metals from Water. *Environ. Sci. Pollut. Res.* **2021**, *28*, 52014–52031. [CrossRef] [PubMed]
34. Mehdipour-Ataei, S.; Hatami, M. Synthesis and Characterization of Novel Heat Resistant Poly(Amide Imide)S. *Eur. Polym. J.* **2005**, *41*, 2010–2015. [CrossRef]
35. Pali-Casanova, R.d.J.; Yam-Cervantes, M.A.; Zavala-Loría, J.d.C.; Loría-Bastarrachea, M.I.; Aguilar-Vega, M.d.J.; Dzul-López, L.A.; Sámano-Celorio, M.L.; Crespo-álvarez, J.; García-Villena, E.; Agudo-Toyos, P.; et al. Effect of Sulfonic Groups Concentration on IEC Properties in New Fluorinated Copolyamides. *Polymers* **2019**, *11*, 1169. [CrossRef]
36. Ngadiwiyana; Gunawan; Prasetya, N.B.A.; Kusworo, T.D.; Susanto, H. Synthesis and Characterization of Sulfonated Poly(Eugenol-Co-Allyleugenol) Membranes for Proton Exchange Membrane Fuel Cells. *Heliyon* **2022**, *8*, e12401. [CrossRef]
37. Pawlicka, A.; Mattos, R.I.; Tambelli, C.E.; Silva, I.D.A.; Magon, C.J.; Donoso, J.P. Magnetic Resonance Study of Chitosan Bio-Membranes with Proton Conductivity Properties. *J. Memb. Sci.* **2013**, *429*, 190–196. [CrossRef]
38. Corona-García, C.; Onchi, A.; Santiago, A.A.; Martínez, A.; Pacheco-Catalán, D.E.; Alfonso, I.; Vargas, J. Synthesis and Characterization of Partially Renewable Oleic Acid-Based Ionomers for Proton Exchange Membranes. *Polymers* **2021**, *13*, 130. [CrossRef]
39. Pasini Cabello, S.D.; Ochoa, N.A.; Takara, E.A.; Mollá, S.; Compañ, V. Influence of Pectin as a Green Polymer Electrolyte on the Transport Properties of Chitosan-Pectin Membranes. *Carbohydr. Polym.* **2017**, *157*, 1759–1768. [CrossRef]
40. Farzin, S.; Johnson, T.J.; Chatterjee, S.; Zamani, E.; Dishari, S.K. Ionomers From Kraft Lignin for Renewable Energy Applications. *Front. Chem.* **2020**, *8*, 562278. [CrossRef]